Chem. Res. Chin. Univ. 2013, 29(2), 299—306 doi: 10.1007/s40242-013-2384-4

Inhibition of CK2 Activity by TCDD *via* Binding to ATP-competitive Binding Site of Catalytic Subunit: Insight from Computational Studies

XU Xian-jin[1], CANNISTRARO Salvatore[2], BIZZARRI Anna-rita[2*], ZENG Yi[1], CHEN Wei-zu[1] and WANG Cun-xin[1*]

1. College of Life Science and Bioengineering, Beijing University of Technology, Beijing 100124, P. R. China;
2. Biophysics and Nanoscience Centre, CNISM, Dipartimento di Biologia ed Ecologia(DEB) Universita della Tuscia, Viterbo 01100, Italy

Abstract Alternative mechanisms of toxic effects induced by 2,3,7,8-tetrachlorodibenzo-*p*-dioxin(TCDD), instead of the binding to aryl hydrocarbon receptor(AhR), have been taken into consideration. It has been recently shown that TCDD reduces rapidly the activity of CK2(casein kinase II) both *in vivo* and *in vitro*. It is found that TCDD has high molecular similarities to the known inhibitors of CK2 catalytic subunit(CK2α). This suggests that TCDD could also be an ATP-competitive inhibitor of CK2α. In this work, docking TCDD to CK2 was carried out based on the two structures of CK2α from maize and human, respectively. The binding free energies of the predicted CK2α-TCDD complexes estimated by the molecular mechanics/Poisson-Boltzmann surface area(MM/PBSA) method are from –85.1 kJ/mol to –114.3 kJ/mol for maize and are from –96.1 kJ/mol to –118.2 kJ/mol for human, which are comparable to those estimated for the known inhibitor and also ATP with CK2α. The energetic analysis also reveals that the van der Waals interaction is the dominant contribution to the binding free energy. These results are also useful for designing new drugs for a target of overexpressing CK2 in cancers.

Keywords Casein kinase II; Dioxin; Inhibitor; Modeling; Binding free energy

1 Introduction

2,3,7,8-Tetrachlorodibenzo-*p*-dioxin(TCDD), a member of dioxin-type chemicals, is regarded as one of the most toxic environmental pollutants and has been proved to be one of the most potent tumor promoters[1—3]. The exposure to TCDD causes a wide variety of effects, such as carcinogenesis, teratogenesis, apoptosis, altering differentiation, and proliferation, while those effects and the sensitivity to TCDD vary greatly among different species[3—7]. However, the mechanisms of TCDD-induced effects are still not completely understood. Most studies focused on the aryl hydrocarbon receptor(AhR), a ligand-dependent transcription factor, which is considered as a high-affinity receptor of TCDD[3,8—10]. Meanwhile, several studies were focused on the alterations of activities of nuclear protein kinases caused by TCDD, in which TCDD reduces rapidly the activity of CK2(casein kinase II) *in vivo* or *in vitro*[11—13]. Significantly, a rapid reduction of the activity of CK2 was observed in short-time(15 min) treatments with TCDD *in vitro*, without a significant decrease of the CK2 protein level[13]. CK2 is distributed ubiquitously in various types of cells and tissues with hundreds of protein targets, functioning in a variety of cell processes including apoptosis, transcription, and cell cycle progression[14—18]. The inactivation of CK2 exposed to TCDD implies that CK2 might also play an important role in the toxic effects of TCDD.

CK2, a heterotetrameric enzyme, consists of two catalytic subunits, CK2α, and two regulatory subunits, CK2β[19]. Recent studies also indicate that free α- and β-subunits exist in mouse tissues with differential subcellular localization and independent nuclear transport[20]. Subunit CK2α is a member of eukaryotic protein kinases(EPKs) superfamily. Proteins from the superfamily phosphorylate special serine, threonine, and tyrosine residues in substrate proteins by transferring the phosphate group from ATP to the terminal hydroxy groups of those three residues. CK2α molecule consists of two domains, a smaller (α+β)-type N-terminal domain and a mainly α-helix C-terminal domain. The N-terminal domain possesses the CK2α/CK2β interaction region. Between the two domains, there is an inter-domain cleft which corresponds to the ATP-binding site(see Fig.1). Since CK2 overexpression was observed in various cancers, it has been considered as a target for cancer therapy[18,21,22]. Several classes of inhibitors have been identified, most of which bind to the ATP-competitive binding site, while

*Corresponding authors. E-mail: bizzarri@unitus.it; cxwangbjut@gmail.com

Received October 11, 2012; accepted November 30, 2012.

Supported by the International Science and Technology Cooperation Program of China(No.2010DFA31710), the National Natural Science Foundation of China(No.10974008), the Doctoral Fund of Innovation from Beijing University of Technology (China), and the Project from the Italian Association for Cancer Research(No.IG10412).

other ligands, more frequently, peptide-based inhibitors, bind to CK2α/CK2β interface near the β4-β5 loop disrupting the formation of CK2 α/β assembly[22].

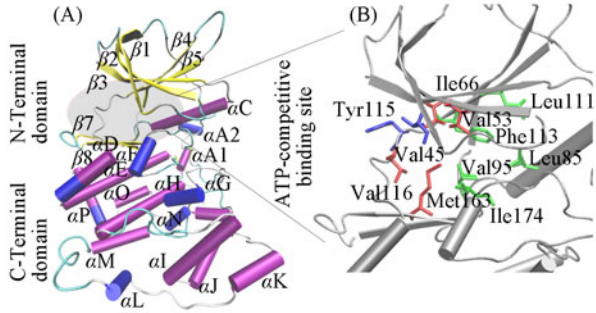

Fig.1 Crystal structure of CK2α

(A) Three dimensional structure of apo-CK2α(from maize, PDB entry: 1jam). The protein consists of a smaller (α+β)-type N-terminal domain and a mainly α-helix C-terminal domain; (B) a zoom-in figure of the ATP-competitive binding site located at the cleft between the two sub-domains. Residues in hydrophobic region I(Leu85, Val95, Leu111, Phe113, and Ile174), adenine region(Val53, Ile66, Val116 and Met163), and hydrophobic region II(Val45 and Tyr115) are represented with the licorice model.

In the present work, we investigated molecular similarities between TCDD and some known ATP-competitive inhibitor of CK2α. TCDD was then docked to CK2α by both global blind docking and local flexible docking based on the structures of CK2α from maize and human, which are characterized by different structural properties with the ATP-binding site of CK2α from human being more flexible than the one from maize. Molecular dynamics(MD) simulations were employed to further refine the predicted CK2α-TCDD complexes. The binding free energies of TCDD to CK2α were calculated by means of molecular mechanics/Poisson-Boltzmann surface area(MM/PBSA) method based on equilibrated MD trajectories[23—27]. As a reference, binding energies of a known inhibitor and ATP with CK2α were also calculated. The results demonstrate that TCDD acts as an inhibitor of CK2α *via* binding to the ATP-competitive binding site. The analysis is not only meaningful to further disclose the toxic effect of TCDD, but also useful for the designing of new drugs targeting the overexpression of CK2 in cancers.

2 Methods

2.1 Molecular Similarity

Molecular similarity principle, which is widely used in drug design, states that the molecules with similar structure tend to have similar properties[28—34]. Here, four molecules from different classes of inhibitors as described in ref.[22], quinalizarin(1,2,5,8-tetrahydroxy-anthraquinone), TBB(4,5,6,7-tetrabromo-1-benzotriazole), DBC(3,8-dibromo-7-hydroxy-4-methylchromen-2-one) and IQA([5-oxo-5,6-dihydro-indolo (1,2-a) quinazolin-7-yl] acetic acid), were chosen for the similarity analysis. The structures and inhibition contant K_i values are listed in Table 1[22]. The 3D structures of small molecules were created by GaussView3, followed by a minimization at the semiempirical AM1 level with Gaussian 03[35]. For considering the structural rigidity of TCDD and the four chosen inhibitors, a rigid-body superimposition and similarity evaluation approach, ShaEP[36], was employed for the molecular similarity calculation in the present work. Simply, TCDD was superimposed on each selected molecule by means of a matching algorithm and then the initial alignments were optimized by maximizing the overlap of the molecules. Two kinds of characters, 3D-shape and electrostatic potential, of the molecules were calculated for comparison. The output values are from 0 to 1 with 0 corresponding to no similarity and 1 corresponding to the same molecules.

Table 1 Molecular similarities of TCDD to the known inhibitors of CK2α

Inhibitor	Structure	Inhibition constant, K_i/(μmol·L^{-1})	Shape similarity	ESP similarity[a]	Average similarity
TCDD	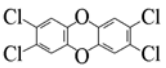	N/A[b]	1.0	1.0	1.0
Quinalizarin	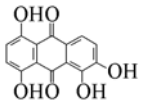	0.05	0.897	0.539	0.718
TBB	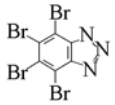	0.40	0.715	0.679	0.697
DBC	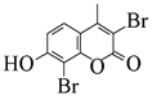	0.06	0.868	0.484	0.676
IQA	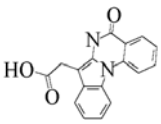	0.40	0.768	0.522	0.645

a. ESP Similarity: Electrostatic potential similarity; *b*. N/A: not available.

2.2 Molecular Docking

The initial coordinates of CK2α were obtained from Protein Data Bank(PDB), whose entries are 1jam(a.a 7-333) for *Zea mays* with apo-form[37] and 3bqc(a.a 3-330) for *H. sapiens* with high resolution[38]. For convenience, we call these two proteins Z_CK2α(from *Zea mays*) and H_CK2α(from *H. sapiens*) for short in the descriptions below. The following

molecular dockings were performed with AutoDock4.2 package[39]. Autodocktools were employed to prepare the systems and the Casteiger partial charges were assigned to the ligand and receptor[40].

First, TCDD was docked to the two CK2α by global blind docking. The proteins were treated as rigid. The maximum number of energy evaluations was set to 2.5×10^7. The grid number of the box was set to 100×120×100 for Z_CK2α and 120×90×100 for H_CK2α with a grid spacing of 0.06 nm, so that the box has enough space to fit the whole receptor and also for the free rotation of the ligand. A hundred complex structures were generated for each docking. The other docking parameters were set to default.

After the global blind docking, we set the box to a grid number of 56×56×60 for the two proteins with a grid spacing of 0.0375 nm, which focus on the ATP-competitive binding site. In a previous review article[22], the known CK2α-inhibitor complex structures were carefully analyzed, in which the ATP-competitive binding cleft was formed by residues Leu85, Val95, Leu111, Phe113, and Ile174(hydrophobic region I), Val53, Ile66, Val116 and Met163(adenine region), and Val45 and Tyr115(hydrophobic region II), for Z_CK2α. In our flexible docking studies, these residues in Z_CK2α and corresponding residues in H_CK2α were treated as flexible residues. The maximum number of energy evaluations was increased to 5×10^7 to make sure that the conformational space could be sufficiently explored. Again, a hundred complex structures were generated for each docking. The sizes of clusters and the estimated free energy of binding(FEB) were used to select potential complex structures from generation results. The FEB here, which was calculated by using a semiempirical free energy force field parameterized on the database of protein-inhibitor complexes[39], is different from the free energy of binding calculated by MM/PBSA method in the following text. The chosen docking poses were used as initial coordinates for the following MD studies.

2.3 Molecular Dynamics Simulation

Molecular dynamics(MD) simulations were carried out by GROMACS4.5.5[41] with GROMOS 43a1 force field[42]. The topology of the ligand was generated by PRODRG server[43]. The structure of the ligand was optimized by Gaussian 03[35] with semiempirical AM1 method and the charges were reassigned by mulliken approach[35,44]. Linear constraint solver (LINCS) algorithm was used to constrain the bond lengths[45]. The velocity rescaling method[46] was used to maintain the temperature at 300 K; CK2α was coupled with TCDD in the same thermostatting group for CK2α-TCDD complexes. The Parrinello-Rahman method[47] was employed to maintain the pressure at 1.01325×10^5 Pa. Short-range electrostatic and van der Waals forces were calculated for all the pairs of a neighbor list with a cutoff radius of 1 nm and updated every 10 steps. Long-range electrostatic interactions were calculated by the particle mesh Evald(PME) method[48]. The integration time step was set to 2 fs and the snapshots of the system were saved every 2 ps. The monomers or the CK2α-TCDD complexes were surrounded by a cubic box of simple charge(SPC) water[49] extending at least 1.0 nm in all the directions from the solute. To neutralize the system, a Cl^- ion was added in the cases of Z_CK2α and Z_CK2α-TCDD complex. First, the systems were minimized by 1000 steps with the steepest descent algorithm, followed by a 200 ps position restrained MD to relax the solvent. Then the systems were heated from 50 K up to 300 K within 500 ps gradient of 50 K. Finally, a 25 ns simulation at a constant temperature of 300 K and a constant pressure of 1.01325×10^5 Pa was carried out for each system. The analyses of the trajectories were performed with the GROMACS software package and the figures of protein structures were created with the VMD program[50].

2.4 MM/PBSA Binding Free Energy

The MM/PBSA method[23,51,52] is an approach to evaluate binding affinities of a complex based on a combination of molecular mechanics with continuum solvent approach. The binding free energies(ΔG_b), of a complex formed by a ligand(L) and a receptor(R) were calculated by MM/PBSA approach as follows:

$$\Delta G_b = G_{RL} - G_R - G_L \tag{1}$$

where each term on the right-hand side is given by

$$G = \langle E_{MM} \rangle + \langle G_{solv} \rangle - \langle TS \rangle \tag{2}$$

where the free energy is decomposed into three terms, molcular mechanics(E_{MM}), solvation contribution(G_{solv}), and entropic contribution(TS). The angle-brackets mean that the value is averaged over a set of snapshots taken from MD trajectory. In the present work, 800 snapshots taken from the last 8 ns equilibrated simulation were used for the binding free energy calculation for each case.

The molecular mechanical energy, E_{MM}, includes three terms, internal energy(E_{int}, where int means bonds, angles, and dihedrals), van der Waals energy(E_{vdW}), and electrostatic component(E_{elec}). The values of these three terms were determined with the same GROMOS 43a1 force field, used in the MD simulations by using GROMACS package. The solvation contribution term, G_{solv}, was calculated *via* MM/PBSA method. The electrostatic component of the solvation free energy(G_{PB}) was determined with the Adaptive Poisson-Boltzmann Solver(APBS) program[53] which numerically solves the Poisson-Boltzmann equation. The atomic charges and radii were set according to the parameters used in MD simulations. The interior dielectric constant for solute was set to 1 and the exterior dielectric constant for water was set to 80[23,25]. The dielectric boundary was determined by a spherical probe with a radius of 0.14 nm. The grid spacing was set to 0.06 nm. The nonpolar component of the solvation free energy (G_{np}) was computed by the solvent-accessible surface area (SASA) approach, $G_{np} = \gamma \times \mathrm{SASA} + \beta$, with γ=2.2 kJ·mol^{-1}·nm^{-2} and β=3.84 kJ/mol[23,54].

The entropic contribution was estimated by the quasi-harmonic analysis[55], which was based on the all-atom covariance matrix. The covariance matrix can be calculated by a standard GROMACS utility from a MD trajectory. The

configurational entropy by this approach is given by the following expression,

$$S_{\mathrm{ho}} = k_{\mathrm{b}} \sum_{i=1}^{3N-6} \left[\frac{\gamma}{e^{\gamma}-1} - \ln\left(1-e^{\gamma}\right) \right] \quad (3)$$

where $\gamma = h / 2\pi\sqrt{1/k_{\mathrm{B}}T\lambda_i}$, h is the Planck constant, k_{B} is the Boltzmann constant, T is the absolute temperature, and λ_i is the eigenvalue of the all-atom mass-weighted covariance matrix of fluctuation $\delta_{ij} = \sqrt{m_i m_j}\left\langle \left(x_i - \langle x_i \rangle\right)\left(x_j - \langle x_j \rangle\right)\right\rangle$.

3 Results and Discussion

3.1 Shape and Electrostatics Similarity

Starting from the knowledge of some small molecules identified as inhibitors for CK2*α*, we have carried out an analysis of molecular similarity between TCDD and these known inhibitors to understand the possible mechanisms of inactivation of CK2 caused by TCDD. In particular, two important characters, 3D-shape and electrostatic potential, for TCDD have been compared to those of the four chosen small molecules, which are known to inhibit the activity of CK2*α* with a very low value of inhibitory constant K_{i}(column in Table 1) by binding to the ATP-competitive binding site. The shape similarity and electrostatic potential similarity(EPS similarity) of TCDD to those of the four inhibitors are reported in column 4 and 5 of Table 1. The quite high value(0.897) of shape similarity between TCDD and quinalizarin indicates that TCDD shares a highly similar 3D shape with this class of inhibitors. Comparing the structures of the two kinds of molecules, TCDD and quinalizarin possess a very similar framework structure with a planar three-member ring. In addition, TCDD also has a high shape similarity to DBC with a similarity value of 0.868. The shape similarity values of the other two inhibitors, TBB and IQA, are a little lower, that is, 0.715 and 0.768, respectively. The ESP similarity results show that TCDD has the highest similarity of electrostatic potential to TBB with a similarity value of 0.679. The high EPS similarity should be due to the benzene ring and the halogen molecules present in both TCDD and TBB. The value of ESP similarity of TCDD to quinalizarin is 0.539, while the one to DBC is relatively low, 0.484. By combining the two characters, the average values of similarity, reported in column 6 in Table 1, show that quinalizarin has the highest molecular similarity of 0.718 compared with TCDD. TCDD also displays a high similarity to the remaining inhibitors with a similarity value higher than 0.64. Since these molecules can bind to the ATP-competitive binding site of CK2*α*, their high molecular similarity to TCDD suggests that it could also be an ATP-competitive inhibitor to CK2*α*.

3.2 Prediction of Binding Site and Binding Modes

Besides the ATP-competitive binding site, CK2*α* has a non-ATP-competitive binding site near the *β*4-*β*5 loop(or called 'secondary binding site') and several ligands have been proved to bind to this region[22]. In the present work, the global blind docking approach was employed to predict the binding site of CK2*α* for TCDD. The clustering analytical results show that TCDD binds to the Z_CK2*α* at ATP-competitive binding site in 99 ones out of total 100 docking structures with a value of FEB around –25.8 kJ/mol. The remaining one binds to a region near the loop between *α*J and *α*K(Fig.1) with an average value of FEB, –23.3 kJ/mol. Significantly, the results of the docking between H_CK2*α* and TCDD show that TCDD binds to the ATP-competitive binding site in all the docking structures with an average value of FEB, –27.3 kJ/mol.

To obtain rational detailed binding patterns between TCDD and CK2*α*, flexible dockings were carried out by considering the flexibility of side chains of residues in the ATP-competitive binding site. 100 docking structures were generated for each case. The generated docking poses were clustered by root mean square(RMS) difference with a value of cutoff, 0.2 nm. As shown in Fig.2(A) and (B), 5 and 11 clusters were generated for Z_CK2*α* and H_CK2*α*, respectively. The occupancies of the top three clusters for Z_CK2*α* are 33%, 10% and 50% with the average values of FEB –24.6, –22.3 and –16.6 kJ/mol, respectively. For convenience, the three docking poses for Z_CK2*α* will be called Z_mol_1, Z_mol_2, and Z_mol_3. The occupancies of the top three clusters for H_CK2*α* are 31%, 15% and 34% with the values of FEB –24.8, –23.0 and –22.7 kJ/mol, respectively. The three docking poses for H_CK2*α* will be called H_mol_1, H_mol_2, and H_mol_3. The six complex conformations(Z_mol_1—3 and H_mol_1—3) were used as initial coordinates for further refinements and studies with MD simulation.

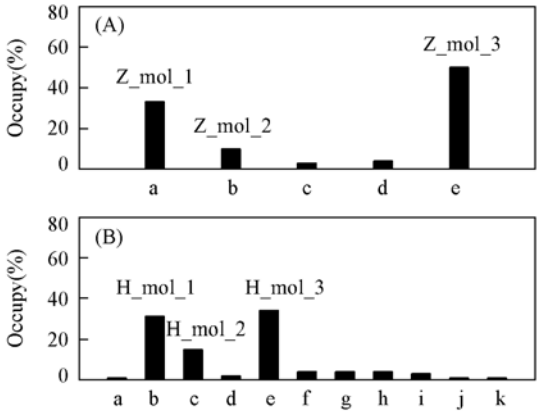

Fig.2 Docking results of TCDD to CK2*α*

(A) TCDD was docked to the CK2*α* from maize; binding energy of clusters a—e were –24.6, –22.3, –19.6, –19.5 and –16.6 kJ/mol; (B) TCDD was docked to the CK2*α* from human. Binding energies of clusters a—k were –27.6, –24.8, –23.0, –22.8, –22.7, –22.7, –21.6, –21.6, –21.4, –18.2 and –18.2 kJ/mol.

3.3 Molecular Dynamics Simulations

To fully consider the flexibility of receptor, which is a critical aspect to recognize, to interact, and to associate with a ligand[56], the CK2*α*-TCDD complexes were subjected to MD runs to refine the flexible docking poses and to reach more favorable binding patterns. To investigate the structural stability of CK2*α* after the ligand binding, the root mean square deviations(RMSD) of the receptor were analyzed. Fig.3(A) and (B) show the backbone RMSD as a function of time for Z_CK2*α* and H_CK2*α*, respectively. For the case of Z_CK2*α*, the

RMSD values of all runs rise to around 0.2 nm after simulations in a short time. Then, Z_mol_1 keeps stable for a long time and increases up to around 0.28 nm at the end of simulation. Z_mol_2 fluctuates around 0.2 nm in the rest of the run while Z_mol_3 keeps rising to about 0.3 nm at 6 ns and fluctuates around 0.28 nm in the remaining simulation. Similar to the case of Z_CK2*α*, the backbone RMSD of three runs of H_CK2*α* increases quickly up to 0.2 nm after simulations. H_mol_1 and H_mol_2 fluctuate around 0.25 nm in the following simulations, while H_mol_3 keeps rising to about 0.3 nm at 7 ns then keeps stable in the rest of simulation. For the six runs, the backbone RMSDs reach stable with values around or lower than 0.3 nm after 7 ns(see Fig.3).

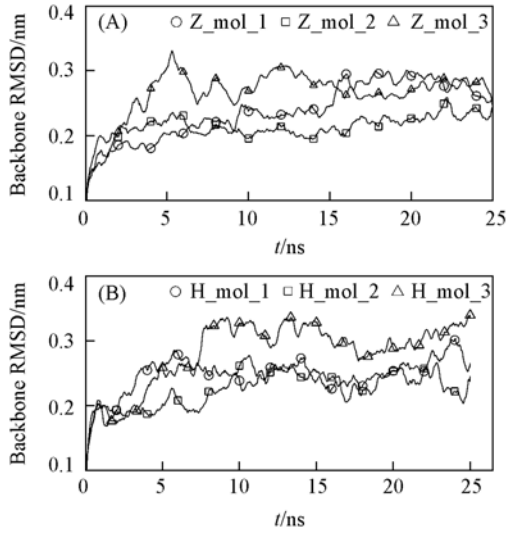

Fig.3 Temporal evolutions of CK2*α*-backbone RMSD

(A) RMSD evolutions of the three models of Z_CK2*α*-TCDD complexes; (B) RMSD evolutions of the three models of H_CK2*α*-TCDD complexes.

The RMSD of TCDD as a function of time with respect to the docking pose has been calculated by superimposing backbone atoms of evolutional conformations on those of the initial structure. As shown in Fig.4(A) for Z_CK2*α*, the RMSDs rapidly increase up to around 0.5 nm in model 1 and keep stable at about 6 ns. Subsequently, the RMSDs decrease to about 0.3 nm at around 9 ns. For the case of Z_mol_2, the RMSDs increase quickly to 0.4 nm after the simulation and then again up to about 0.6 nm at 2 ns. The values keep stable for about 1 ns and then decrease to a low value of around 0.2 nm. Similarly, the RMSDs of Z_mol_3 increase quickly after simulation and keep stable with a low value after fluctuation for several nanoseconds. The RMSD with the high value might correspond to a rearrangement of the binding pocket to search for a more comfortable binding pattern for the ligand. The last part of simulation with low RMSD values for TCDD indicate that the ligand returns near to the initial position after the rearrangement of binding site. Fig.4(B) shows the temporal evolutions of RMSD of TCDD for the three binding modes of H_CK2*α*. Similar to what observed in the case of Z_CK2*α*, the RMSD values for the three models increase rapidly up to around 0.5 nm and stay there for several nanoseconds. The RMSD of TCDD in H_mol_1 rises again after 3 ns and then reaches a new stable arrangement with a higher RMSD value. A similar phenomenon has been observed in the cases of H_mol_2 and H_mol_3, in which the RMSDs rise again at around 8 and 9.7 ns, respectively, by successively reaching new stable situations. These might indicate that TCDD has found out a new position upon the rearrangement of the binding pocket. Comparing the last conformation from each run to its initial docking pose, we do find large moving of TCDD in the binding pocket of the three binding modes for H_CK2*α*. This might be due to the higher flexibility of the ATP-binding site of H_CK2*α* compared with that of Z_CK2*α*.

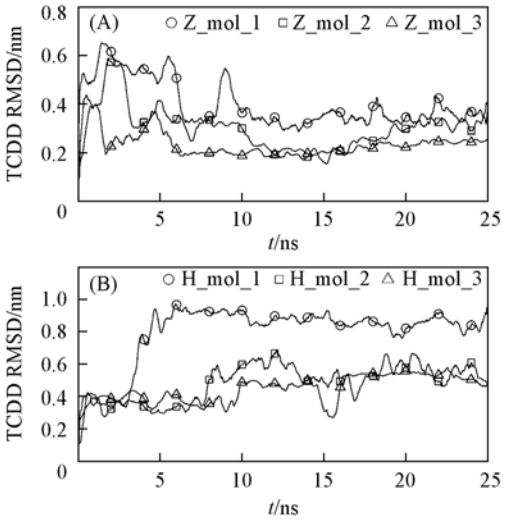

Fig.4 Temporal evolutions of RMSD for TCDD

(A) Z_CK2*α*-TCDD complexes; (B) H_CK2*α*-TCDD complexes.

3.4 Energetic Analysis of CK2*α*-ligand Complexes

The binding free energies, together with the single contributions from the single terms, were calculated by the MM/PBSA approach for the predicted CK2*α*-TCDD complexes with the results reported in Table 2. Calculations of the molecular mechanical contribution(including ΔE_{int}, ΔE_{elec}, and ΔE_{vdW}) and of the solvation contribution(including ΔG_{PB} and ΔG_{np}) were carried out from snapshot structures(monomers and complex) derived from related single MD trajectories. Since the monomers have the same conformations in bound and unbound states, the contributions from the internal component of the molecular mechanics have been put to zero(ΔE_{int}=0). The configurational entropies were estimated by quasi-harmonic approximation. The final values of binding free energy(ΔG_b) range from –85.1 kJ/mol to –114.3 kJ/mol for Z_CK2*α*-TCDD and from –96.1 kJ/mol to –118.2 kJ/mol for H_CK2*α*-TCDD. Interestingly, the models with the lowest energy for the two cases, Z_mol_3 and H_mol_3, are not the best model predicted by flexible docking(Fig.2). This could be due to the changes as induced by the rearrangements of the docking poses during MD simulations, especially in the case of H_CK2*α*, in which large movements of the ligand were observed.

From Table 2, it comes out that the contribution from the electrostatic component of the molecular-mechanical energy(ΔE_{elec}) is quite small for both Z_CK2*α*-TCDD and H_CK2*α*- TCDD with values from –0.1 kJ/mol to –2.9 kJ/mol. The van der Waals contributions(ΔE_{vdW}), with values from

Table 2 Binding free energies of TCDD, quinalizarin and ATP with CK2α*

Complex	ΔE_{elec}/(kJ·mol^{-1})	ΔE_{vdW}/(kJ·mol^{-1})	ΔG_{PB}/(kJ·mol^{-1})	ΔG_{np}/(kJ·mol^{-1})	$-T\Delta S$/(kJ·mol^{-1})	ΔG_b/(kJ·mol^{-1})
Z_mol_1-TCCD	–0.4(1.2)	–123.1(12.3)	34.4(8.9)	–5.1(0.8)	9.1	–85.1
Z_mol_2-TCCD	–1.4(2.2)	–176.9(10.0)	84.5(12.2)	–9.3(0.6)	12.6	–90.5
Z_mol_3-TCCD	–0.1(1.0)	–180.4(9.9)	64.3(12.0)	–9.7(0.6)	11.6	–114.3
H_mol_1-TCCD	–0.6(1.7)	–146.3(8.1)	48.9(11.2)	–8.0(0.7)	9.9	–96.1
H_mol_2-TCCD	–1.6(1.4)	–144.1(9.6)	42.7(11.8)	–7.6(1.0)	8.8	–101.8
H_mol_3-TCCD	–2.9(0.9)	–180.4(8.9)	64.5(10.6)	–10.2(0.5)	10.8	–118.2
CK2α-Quinalizarin	–17.9(6.8)	–176.8(10.6)	53.4(26.5)	–7.5(0.58)	37.4	–111.4
CK2α-ATP	–1268.8(49.1)	–124.2(20.2)	680.9(203.8)	–14.9(0.6)	55.9	–671.1

* The values in the parentheses are standard deviations of average.

–123.1 kJ/mol to –180.4 kJ/mol for Z_CK2α-TCDD and from –144.1 kJ/mol to –180.4 kJ/mol for H_CK2α-TCDD, give dominant contributions to the final binding free energies. The solvation free energy, consisting of the electrostatic component(ΔG_{PB}) and the nonpolar component(ΔG_{np}), is characterized, in all the models, by relatively large positive value of ΔG_{PB}, from 34.4 kJ/mol to 84.5 kJ/mol, with negative contributions to the binding free energy. This reveals the unfavorable rearrangement of the receptor from the electrostatics of solvation during the formation of the complex. Differently, contributions from ΔG_{np} are positive for all the models with values from –5.1 kJ/mol to –10.2 kJ/mol. The results of $T\Delta S$ in Table 2 show that the configurational entropic component is always unfavorable to the binding.

Therefore, all the binding modes for the two cases are characterized by the low values of binding free energy, with the Z_mol_3 being the lowest one for Z_CK2α and the H_mol_3 for H_CK2α. The contribution from each term displays a similar trend for all binding modes. The favorable formations of the complexes are mainly driven by the van der Waals energy (ΔE_{vdW}) and partly by the nonpolar contributions of solvation(ΔG_{np}). This is in agreement with the hydrophobic properties of TCDD and also the ATP-competitive binding site of CK2α which consists of two hydrophobic regions and an adenine region(see Fig.1).

These results have been obtained by using a dielectric constant value of 1 for the protein interior according to the literature[27—30]. In the other MM/PBSA studies, higher values, like 4 and 8, have been used for ε[57—59]. Therefore, we have also tested the values 4 and 8. The results show that smaller values of ΔG_{PB} were obtained for larger values of ε(data not shown). In our cases, the value of ΔG_{PB} is positive for each model with unfavorable contribution to the final binding free energy. The smaller value of ΔG_{PB}, which means the lower value of final binding free energy, indicates that different values of ε do not substantially change our final results. In addition, this is in agreement with previous studies, showing that the absolute value of the electrostatic component of solvation is roughly inversely proportional to the value of ε[57,58].

In the above MM/PBSA calculations, snapshots of monomers, CK2α and TCDD, and the complex were taken from the same run of CK2α-TCDD complex. Meanwhile, we also calculated binding free energies based on the snapshots taken from the separate trajectories of monomers(CK2α or TCDD). In the latter case, large standard deviations, comparable to or even larger than the average values, have been observed for the various energy components(data not shown). The result is in agreement with that observed in several previous studies[58,60] calculating binding free energies of protein-protein complex or protein-ligand complex based on MM/PBSA method.

In order to directly compare to known inhibitors and ATP, we also calculated the binding free energies of Quinalizarin and ATP to CK2α. The PDB 3fl5 was used for the coordinate of CK2α-Quinalizarin complex[61]. The original structure of CK2α in complex with AMPPNP and Mg^{2+} was taken from PDB with entry of 1daw[62]. The CK2α-ATP complex structure was obtained by replacing the nitrogen atom in the triphosphate chain of AMPPNP with oxygen atom. 10 ns simulation with the same setting described in the Section 2.4 was carried out for the two complexes. The two simulations reached equilibrium within 3 ns with RMSDs of both the backbone of the protein and the ligand lower than 0.3 nm. The MM/PBSA calculations were based on 500 snapshots extracted from the last 5 ns simulations. The results are also reported in Table 2.

The binding free energy of Quinalizarin to CK2α is –111.4 kJ/mol, which is comparable with the values of CK2α-TCDD complexes(see Table 2). Similar to that observed from CK2α-TCDD complexes, the ΔE_{vdW} has the dominant contribution to the binding with a value of –176.8 kJ/mol. The contributions from ΔG_{PB} and ΔG_{np} are 53.4 and –7.5 kJ/mol, respectively. Differently, larger positive contributions from the term of ΔE_{elec} were observed, with a value of –17.9 kJ/mol mainly due to the hydroxyl groups. Besides, the entropic term has a larger negative contribution(37.4 kJ/mol) to the ligand binding.

For the CK2α-ATP complex, similar to those observed from CK2α-TCDD and CK2α-Quinalizarin complexes, the ΔE_{vdW} and ΔG_{np} have positive contributions to the binding with values of –124.2 and –14.9 kJ/mol, respectively. The contribution from entropic term is negative with a value of 55.9 kJ/mol, which is larger than those for TCDD and Quinalizarin. Differently, the contributions from the electrostatic terms, ΔE_{elec} and ΔG_{PB}, are dominant to the final binding free energy, with values of –1268.8 and 680.9 kJ/mol, respectively. It should be noted that the large values of the electrostatic terms are mainly from the contributions of two Mg^{2+} ions, which are critical to the ATP's binding[62]. Finally, the calculated binding free energy of ATP to CK2α is –671.1 kJ/mol, which is 6-fold lower than those of TCDD and Quinalizarin to CK2α.

3.5 Analysis of the Predicted Complexes

The structure of each model averaged over last 100 ps is shown in Fig.5. The three predicted models of Z_CK2α-TCDD

display different binding patterns. In Z_mol_1, TCDD binds to the region between $\beta1/\beta2$ loop and αF, located at the edge of the ATP-competitive binding site(Fig.1). The binding region in Z_mol_2 is near to that found in Z_mol_1, while the orientation of TCDD is turned back about 90° with one end inserted into the cleft between αD and αF. TCDD in Z_mol_3 binds into much deeper inside the ATP-competitive binding site with respect to the first two models. For the case of H_CK2α shown in Fig.5(B), TCDD binds to a region near to the adenine region and the hydrophobic region II of the ATP-competitive binding site in H_mol_1 and H_mol_2. These two models share a similar binding pattern with a slight rotation for TCDD. Similar to that in Z_mol_3, the binding region of TCDD in H_mol_3 is deep inside the ATP-competitive binding site. The distinct binding patterns with low values of binding free energy suggest that some of conformations might be trapped into the local minimal states in the free energy landscape of the CK2α-TCDD complex. The state of the global minimum of the free energy is often corresponding to the native structure of the complex. Here, we would like to further illustrate the best predicted model, which has the lowest value of binding free energy in each case, Z_mol_3 and H_mol_3.

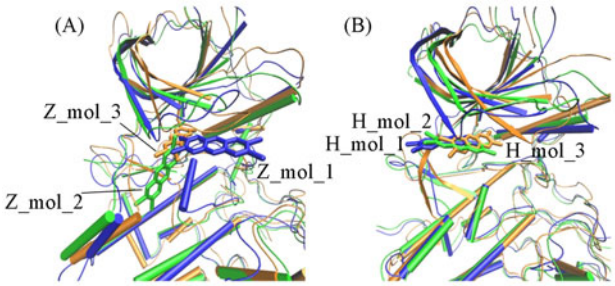

Fig.5 Predicted binding modes of TCDD to CK2α

(A) Z_CK2α-TCDD complexes; (B) H_CK2α-TCDD complexes. The proteins were superimposed based on backbone atoms.

The 3D structures of ligand and its contact residues, determined by LIGPLOT program[63] with a default cutoff of 0.39 nm, are illustrated in Fig.6(A) and (B) for Z_mol_3 and H_mol_3, respectively. In Z_mol_3, one end of TCDD inserts into the hydrophobic region I(see ATP-competitive binding site illustrated in Fig.1) by interacting with Phe113, and Ile174. The ligand also partly binds to the adenine region with interactions with Val53, Ile66 and Met163. However, we did not find any interactions of it with the hydrophobic region II, which consists of Val45 and Tyr115. Besides the interactions with theses hydrophobic residues, TCDD was found to interact with charged or hydrophilic residues. The detailed interactions of protein-ligand in H_mol_3 are shown in Fig.6(B). It is noticed that several contact residues in H_mol_3, such as Val53, Lys68, Phe113, Met163, and Asp175, also appeared in the contact residues in Z_mol_3. Similar to that in Z_mol_3, TCDD plugs in the hydrophobic region I with one end and also binds to adenine region with interactions with Val53, Val66, and Met163. Differently, the other end of TCDD in H_mol_3 is in contact with hydrophobic region II by touching Leu45. A hydrophobic residue Trp176 and three charged residues, Arg47, Lys68 and Asp175, are also of the contact residues.

In the two best models, Z_mol_3 and H_mol_3, the ligand

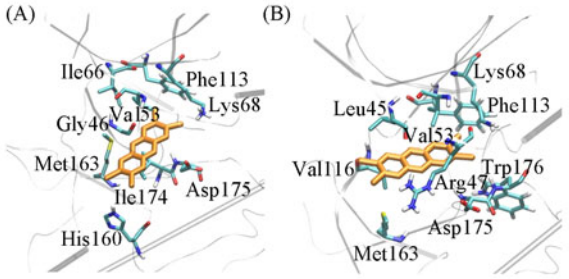

Fig.6 Detailed interactions of the best predicted model

The contact residues are represented with the licorice model, for Z_mol_3(A) and H_mol_3(B). Residues are determined by the LIGPLOT program with a default cutoff of 0.39 nm.

mainly binds to the hydrophobic and adenine regions in the ATP-competitive binding site, in agreement with the finding obtained from the MM/PBSA analysis, showing that the dominant contribution to the final binding free energy comes from van der Waals component. It is found out that the electrostatic component of solvation(ΔG_{PB}) has the negative contribution to the binding free energy. This might be due to the unfavorable contacts of ligand with several charged residues near the ATP-competitive binding site.

4 Conclusions

Starting from the evidence that the activity of CK2 can be rapidly reduced by TCDD both *in vivo* and *in vitro*, we have analyzed the molecular similarities between TCDD and some known ATP-competitive inhibitors of CK2α. It is found that TCDD shares high 3D shape and electrostatic potential similarities with the selected CK2α inhibitors. Docking studies between the two crystal structures of CK2α from maize and human and TCDD have allowed us to show that TCDD binds to the ATP-competitive binding site of CK2α. Flexible docking, followed by MD simulation, has been carried out to reach more favourable binding patterns for the CK2α-TCDD complexes. The binding free energy, calculated by MM/PBSA method, of TCDD to CK2α is comparable with that of known inhibitor and ATP also. The detailed energetic analysis reveals that the TCDD binding processes are driven by nonpolar forces. The detailed analysis of the predicted binding modes shows that TCDD binds to the hydrophobic and adenine regions of ATP-competitive binding site. The study can help us to further understand the mechanism of toxic effects of TCDD and it could be useful for designing new drugs targeting overexpression of CK2 in related cancers.

References

[1] Pitot H. C., Goldsworthy T., Campbell H. A., Poland A., *Cancer Res.*, **1980**, *40*, 3616

[2] Poland A., Knutson J. C., *Annu. Rev. Pharmacol. Toxicol.*, **1982**, *22*, 517

[3] Mandal P. K., *J. Comp. Physiol. B*, **2005**, *175*, 221

[4] Huff J., Lucier G., Tritscher A., *Annu. Rev. Pharmacol. Toxicol.*, **1994**, *34*, 343

[5] Kamath A. B., Xu H., Nagarkatti P. S., Nagarkatti M., *Toxicol. Appl. Pharmacol.*, **1997**, *142*, 367

[6] Pryputniewicz S. J., Nagarkatti M., Nagarkatti P. S., *Toxicology*, **1998**, *129*, 211

[7] Lai Z. W., Fiore N. C., Gasiewicz T. A., Silverstone A. E., *Toxicol. Appl. Pharm.*, **1998**, *149*, 167

[8] Fernandez-Salguero P. M., Hilbert D. M., Rudikoff S., Ward J. M., Gonzalez F. J., *Toxicol. Appl. Pharmacol.*, **1996**, *140*, 173

[9] Dietrich C., Kaina B., *Carcinogenesis*, **2010**, *31*, 1319

[10] Hankinson O., *Annu. Rev. Pharmacol. Toxicol.*, **1995**, *35*, 307

[11] Enan E., Matsumura F., *Biochem. Pharmacol.*, **1995**, *50*, 1199

[12] Enan E., El-Sabeawy F., Scott M., Overstreet J., Lasley B., *Toxicol. Appl. Pharmacol.*, **1998**, *151*, 283

[13] Ashida H., Nagy S., Matsumura F., *Biochem. Pharmacol.*, **2000**, *59*, 741

[14] Pinna L. A., Allende J. E., *Cell Mol. Life Sci.*, **2009**, *66*, 1795

[15] St-Denis N. A., Litchfield D. W., *Cell Mol. Life Sci.*, **2009**, *66*, 1817

[16] Filhol O., Cochet C., *Cell Mol. Life Sci.*, **2009**, *66*, 1830

[17] Dominguez I., Sonenshein G. E., Seldin D. C., *Cell Mol. Life Sci.*, **2009**, *66*, 1850

[18] Trembley J. H., Wang G., Unger G., Slaton J., Ahmed K., *Cell Mol. Life Sci.*, **2009**, *66*, 1858

[19] Niefind K., Raaf J., Issinger O. G., *Cell Mol. Life Sci*., **2009**, *66*, 1800

[20] Kramerov A. A., Ljubimov A. V., *Exp. Eye. Res.*, **2012**, *101*, 111

[21] Guerra B., Issinger O. G., *Curr. Med. Chem.*, **2008**, *15*, 1870

[22] Battistutta R., *Cell Mol. Life Sci.*, **2009**, *66*, 1868

[23] Srinivasan J., Cheatham T. E., Cieplak P., Kollman P. A., Case D. A., *J. Am. Chem. Soc*., **1998**, *120*, 9401

[24] Massova I., Kollman P. A., *J. Am. Chem. Soc.*, **1999**, *121*, 8133

[25] Chong L. T, Duan Y., Wang L., Massova I., Kollman P. A., *P. Natl. Acad. Sci. USA*, **1999**, *96*, 14330

[26] Massova I., Kollman P. A., *Perspect. Drug Discov*., **2000**, *18*, 113

[27] Hou T., Wang J., Li Y., Wang W., *J. Chem. Inf. Model.*, **2011**, *51*, 69

[28] Hendrickson J. B., *Science*, **1991**, *252*, 1189

[29] Martin Y. C., Kofron J. L., Traphagen L. M., *J. Med. Chem.*, **2002**, *45*, 4350

[30] Bender A., Glen R. C., *Org. Biomol. Chem.*, **2004**, *2*, 3204

[31] Maldonado A. G., Doucet J. P., Petitjean M., Fan B. T., *Mol. Divers*., **2006**, *10*, 39

[32] Hu S. Q., Mi S. Q., Jia X. L., Guo A. L., Chen S. H., Zhang J., Liu X. Y., *Chem. J. Chinese Universities*, **2011**, *32*(10), 2402

[33] Zhu J., Sheng C. Q., Zhang M., Song Y. L., Chen J., Yu J. X., Yao J. Z., Miao Z. Y., Zhang W. N., *Chem. J. Chinese Universities*, **2006**, *27*(2), 287

[34] Wang J. G., Fu X. L., Wang Y. M., Ma Y., Li Z. M., Zhang Z. X., *Chem. J. Chinese Universities*, **2003**, *24*(11), 2010

[35] Frisch M. J., Trucks G. W., Schlegel H. B., Scuseria G. E., Robb M. A., Cheeseman J. R., Montgomery J. A. Jr., Vreven T., Kudin K. N., Burant J. C., Millam J. M., Iyengar S. S., Tomasi J., Barone V., Mennucci B., Cossi M., Scalmani G., Rega N., Petersson G. A., Nakatsuji H., Hada M., Ehara M., Toyota K., Fukuda R., Hasegawa J., Ishida M., Nakajima T., Honda Y., Kitao O., Nakai H., Klene M., Li X., Knox J. E., Hratchian H. P., Cross J. B., Bakken V., Adamo C., Jaramillo J., Gomperts R., Stratmann R. E., Yazyev O., Austin A. J., Cammi R., Pomelli C., Ochterski J. W., Ayala P. Y., Morokuma K., Voth G. A., Salvador P., Dannenberg J. J., Zakrzewski V. G., Dapprich S., Daniels A. D., Strain M. C., Farkas O., Malick D. K., Rabuck A. D., Raghavachari K., Foresman J. B., Ortiz J. V., Cui Q., Baboul A. G., Clifford S., Cioslowski J., Stefanov B. B., Liu G., Liashenko A., Piskorz P., Komaromi I., Martin R. L., Fox D. J., Keith T., Al-Laham M. A., Peng C. Y., Nanayakkara A., Challacombe M., Gill P. M. W., Johnson B., Chen W., Wong M. W., Gonzalez C., Pople J. A., *Gaussian 03*, *Revision C02*, Gaussian Inc., Wallingford CT, **2004**

[36] Vainio M. J., Puranen J. S., Johnson M. S., *J. Chem. Inf. Model.*, **2009**, *49*, 492

[37] Battistutta R., De Moliner E., Sarno S., Zanotti G., Pinna L. A., *Protein Sci.*, **2001**, *10*, 2200

[38] Raaf J., Klopffleisch K., Issinger O. G., Niefind K., *J. Mol. Biol.*, **2008**, *377*, 1

[39] Morris G. M., Huey R., Lindstrom W., Sanner M. F., Belew R. K., Goodsell D. S., Olson A. J., *J. Comput. Chem.*, **2009**, *30*, 2785

[40] Gasteiger J., Marsili M., *Tetrahedron*, **1980**, *36*, 3219

[41] Hess B., Kutzner C., van der Spoel D., Lindahl E., *J. Chem. Theory Comput.*, **2008**, *4*, 435

[42] van der Spoel D., Lindahl E., Hess B., Groenhof G., Mark A. E., Berendsen H. J. C., *J. Comput. Chem.*, **2005**, *26*, 1701

[43] Schuttelkopf A. W., van Aalten D. M. F., *Acta Crystallogr. D*, **2004**, *60*, 1355

[44] Lemkul J. A., Allen W. J., Bevan D. R., *J. Chem. Inf. Model.*, **2010**, *50*, 2221

[45] Hess B., Bekker H., Berendsen H. J. C., Fraaije J. G. E. M., *J. Comput. Chem.*, **1997**, *18*, 1463

[46] Bussi G., Donadio D., Parrinello M., *J. Chem. Phys.*, **2007**, *126*, 014101

[47] Parrinello M., Rahman A., *J. Appl. Phys.*, **1981**, *52*, 7182

[48] Essmann U., Perera L., Berkowitz M. L., Darden T., Lee H., Pedersen L. G., *J. Chem. Phys.*, **1995**, *103*, 8577

[49] Berendsen H. J. C., Grigera J. R., Straatsma T. P., *J. Phys. Chem.*, **1987**, *91*, 6269

[50] Humphrey W., Dalke A., Schulten K., *J. Mol. Graph. Model.*, **1996**, *14*, 33

[51] Wang J. M., Hou T. J., Xu X. J., *Curr. Comput. Aided Drug Des.*, **2006**, *2*, 287

[52] Kollman P. A., Massova I., Reyes C., Kuhn B., Huo S., Chong L., Lee M., Lee T., Duan Y., Wang W., *Accounts Chem. Res*., **2000**, *33*, 889

[53] Baker N. A., Sept D., Joseph S., Holst M. J., McCammon J. A., *P. Natl. Acad. Sci. USA*, **2001**, *98*, 10037

[54] Sitkoff D., Sharp K. A., Honig B., *J. Phys. Chem.*, **1994**, *98*, 1978

[55] Andricioaei I., Karplus M., *J. Chem. Phys.*, **2001**, *115*, 6289

[56] Sousa S. F., Fernandes P. A., Ramos M. J., *Proteins*, **2006**, *65*, 15

[57] Archontis G., Simonson T., *J. Am. Chem. Soc.*, **2001**, *123*, 11047

[58] Basdevant N., Weinstein H., Ceruso M., *J. Am. Chem. Soc.*, **2006**, *128*, 12766

[59] Santini S., Bizzarri A. R., Cannistraro S., *J. Mol. Recognit.*, **2011**, *24*, 1043

[60] Swanson J. M., Henchman R. H., McCammon J. A., *Biophys. J.*, **2004**, *86*, 67

[61] Cozza G., Mazzorana M., Papinutto E., Bain J., Elliott M., Di Maira G., Gianoncelli A., Pagano M. A., Sarno S., Ruzzene M., Battistutta R., Meggio F., Moro S., Zagotto G., Pinna L. A., *Biochem. J.*, **2009**, *421*, 387

[62] Niefind K., Putter M., Guerra B., Issinger O. G., Schomburg D., *Nat. Struct. Biol.*, **1999**, *6*, 1100

[63] Wallace A. C., Laskowski R. A., Thornton J. M., *Protein Eng.*, **1995**, *8*, 127